

Electronic Supplementary Information for:

## Natural abundance solid-state $^{95}\text{Mo}$ MAS NMR of $\text{MoS}_2$ reveals precise $^{95}\text{Mo}$ anisotropic parameters from its central and satellite transitions

Hans J. Jakobsen,<sup>\*a</sup> Henrik Bildsøe,<sup>a</sup> Jørgen Skibsted,<sup>a</sup> Michael Brorson<sup>b</sup> and  
Kjeld Schaumburg<sup>c</sup>

<sup>a</sup> *Instrument Centre for Solid-State NMR Spectroscopy  
Interdisciplinary Nanoscience Center (iNANO)*

*Department of Chemistry, Aarhus University, DK-8000 Aarhus C, Denmark*

<sup>b</sup> *Haldor Topsøe A/S, Nymøllevej 55, DK-2800 Lyngby, Denmark*

<sup>c</sup> *CISMI, Roskilde University, Universitetsvej 1, DK-4000 Roskilde, Denmark*

### ESI Contents

Experimental Section.....	Page S2
Experimental, Material.....	Page S2
Experimental, Solid-state $^{95}\text{Mo}$ MAS NMR spectroscopy.....	Page S2
Experimental, Spectral analysis.....	Page S3
Solid-state $^{95}\text{Mo}$ MAS NMR spectra of $\text{MoS}_2$ at 14.1 T.....	Page S4
Simulated solid-state $^{95}\text{Mo}$ MAS NMR spectra of $\text{MoS}_2$ at high field.....	Page S5
Effect of spinning frequency on $^{95}\text{Mo}$ MAS spectra of $\text{MoS}_2$ at 19.6 T.....	Page S6
Conclusion.....	Page S7
References.....	Page S7
Figure S1: The layer structure of $\text{MoS}_2$ .....	Page S8
Figure S2: First $^{95}\text{Mo}$ MAS NMR spectrum for the CT in $\text{MoS}_2$ (see text).....	Page S9
Figure S3: Second $^{95}\text{Mo}$ MAS NMR spectrum (CT and inner STs) of $\text{MoS}_2$ .....	Page S10
Figure S4: Expansion for the CT in Figure S3.....	Page S11
Figure S5: Simulations of the influence of the $\chi$ angle on the CT $^{95}\text{Mo}$ MAS spectrum... Page S12	
Figure S6: Simulated $^{95}\text{Mo}$ MAS NMR spectra of $\text{MoS}_2$ at three magnetic fields.....	Page S13
Figure S7: Expansions for the CT in the three spectra of Figure S6.....	Page S14
Figure S8: Effect of spinning frequency on the 19.6 T $^{95}\text{Mo}$ MAS spectrum of $\text{MoS}_2$ ... Page S15	
Figure S9: Expansions for the CT in the three spectra of Figure S8.....	Page S16

## 1. Experimental

### 1.1 Material

The molybdenite mineral sample of MoS<sub>2</sub> was purchased from Fluka (69680, lot 1308621, code 34407123) and originates from Arizona, USA. Identity was checked by powder X-ray diffraction and by <sup>95</sup>Mo MAS NMR spectroscopy as performed in the present article and described below. The layer structure of MoS<sub>2</sub> is displayed Figure S1.

### 1.2 Solid-state <sup>95</sup>Mo MAS NMR spectroscopy

The <sup>95</sup>Mo MAS NMR experiments were performed on a Varian Direct Drive VNMRS-600 spectrometer at the *Instrument Centre for Solid-State NMR Spectroscopy*, Aarhus, Denmark, operating at 39.03 MHz and equipped with an Oxford Instruments 14.1 T wide-bore magnet. The experiments employed a Varian Chemagnetics double-resonance T3<sup>®</sup> MAS probe for 7.5 mm rotors. The magic angle of  $\theta = 54.736^\circ$  was adjusted to the highest possible precision ( $\leq \pm 0.005^\circ$ ) by <sup>14</sup>N MAS NMR at the nearby frequency of 43.34 MHz, using a sample of NH<sub>4</sub>H<sub>2</sub>PO<sub>4</sub>, as described elsewhere.<sup>1</sup> The sample of MoS<sub>2</sub> was spun at a MAS frequency of  $\nu_r = 5000$  Hz with a high precision ( $< 0.5$  Hz) in  $\nu_r$ , employing the experimental setup, combined with a Varian/Chemagnetic MAS speed controller, as recently described.<sup>2</sup> Rf field strengths were calibrated using an aqueous solution of 2.0 M Na<sub>2</sub>MoO<sub>4</sub> and a flip angle of 90° could be achieved using a pulse width  $\text{pw}(90)_{\text{liquid}} = 6.8 \mu\text{s}$  for the 7.5 mm rotor. This corresponds to a rf field strength  $\gamma B_1/2\pi = 37$  kHz, a field strength used for all experiments in this study. Thus, the pulse width for a 90° ‘solids’ pulse for <sup>95</sup>Mo is given by  $\text{pw}(90)_{\text{solid}} = \text{pw}(90)_{\text{liquid}}/(I + 1/2) = 2.3 \mu\text{s}$ . The <sup>95</sup>Mo signal from the aqueous solution of 2.0 M Na<sub>2</sub>MoO<sub>4</sub> was also used as external reference. The first experiment performed in this study on MoS<sub>2</sub> used a spectral width of 1.25

MHz, a pulse width  $pw = 2.5 \mu\text{s}$  (corresponding to a 'liquids' flip angle of  $33^\circ$  or a 'solids' flip angle of about  $90^\circ$ ) and a relaxation delay of only 1.0 s. For the second and final experiment, performed in this preliminary  $^{95}\text{Mo}$  MAS NMR study on  $\text{MoS}_2$ , the pulse width was reduced to  $pw = 1.0 \text{ s}$  (corresponding to a 'liquid-pulse' flip-angle of  $13^\circ$  or a 'solids' flip angle of  $40^\circ$ ), a relaxation delay of 4.0 s and 82000 scans (i.e., 3.8 days of spectrometer time), which correspond to the  $^{95}\text{Mo}$  MAS NMR spectrum presented and discussed in Fig. 1a of the communication for this work.

### 1.3 Spectral Analysis

The natural abundance  $^{95}\text{Mo}$  MAS NMR spectra of the  $+1/2 \leftrightarrow -1/2$  central transition (CT) and the two  $\pm 3/2 \leftrightarrow \pm 1/2$  satellite transitions (STs) for the molybdenite mineral sample of  $\text{MoS}_2$  have been analyzed using the STARS simulation software package. STARS (SpecTrum Analysis for Rotating Solids) was developed in our laboratory several years ago<sup>3-5</sup>. The original version of STARS was early on incorporated into Varian's VNMR software for SUN Microsystem computers and has been available from Varian Inc as part of their VNMR Solids software package.<sup>5</sup> The present version of STARS used here has been intensively upgraded during the past few years and is capable of handling spectral parameters (i.e., quadrupole coupling ( $C_Q, \eta_Q$ ), chemical shift ( $\delta_{\text{iso}}, \delta_\sigma, \eta_\sigma$ ), and Euler angles ( $\psi, \chi, \zeta$ ) relating the relative orientation for these two interactions) for up to eight different nuclear sites in the optimization of a fit to an experimental spectrum. In addition to these spectral parameters, the program can also include (i) deviation from the magic angle, (ii) rf bandwidth, (iii) rf offset, (iv) jitter in spinning frequency,<sup>2</sup> and (v) the linewidths (Lorentzian and/or Gaussian) in the iterative fitting procedure. This upgraded version of STARS has been incorporated into both the Varian VNMRJ software running on SUN Microsystems Ultra-5 workstations and the VNMRJ software running on a Linux RedHat PC. By including the magic-angle setting and jitter in spinning frequency in the

iteration showed, that upon sample change, the magic angle had increased by  $0.02^\circ$  from its exact value of  $54.736^\circ$ , while the jitter in spinning frequency was less than 1.0 Hz.

The quadrupole coupling and CSA parameters are defined by

$$C_Q = eQV_{zz} / h \quad \eta_Q = (V_{yy} - V_{xx}) / V_{zz} \quad (1)$$

$$\delta_\sigma = \delta_{\text{iso}} - \delta_{zz} \quad \eta_\sigma = (\delta_{xx} - \delta_{yy}) / \delta_\sigma \quad (2)$$

$$\delta_{\text{iso}} = (1/3)(\delta_{xx} + \delta_{yy} + \delta_{zz}) = (1/3)\text{Tr}(\delta) \quad (3)$$

using the convention

$$|\lambda_{zz} - (1/3)\text{Tr}(\lambda)| \geq |\lambda_{xx} - (1/3)\text{Tr}(\lambda)| \geq |\lambda_{yy} - (1/3)\text{Tr}(\lambda)| \quad (4)$$

for the principal elements ( $\lambda_{\alpha\alpha} = V_{\alpha\alpha}$ ,  $\delta_{\alpha\alpha}$ ) of the two tensors. The relative orientation of the two tensors is described by the three Euler angles ( $\psi$ ,  $\chi$ ,  $\zeta$ ) which correspond to positive rotations of the CSA tensor around  $\delta_{zz}$  ( $\psi$ ), the new  $\delta_{yy}$  ( $\chi$ ), and the final  $\delta_{zz}$  ( $\zeta$ ) axis.

## 2. Solid-state $^{95}\text{Mo}$ MAS NMR spectra of $\text{MoS}_2$ at 14.1 T

As described above in the experimental section, the first experimental  $^{95}\text{Mo}$  MAS NMR spectrum acquired in this preliminary investigation on  $\text{MoS}_2$  used a spectral width of 1.25 MHz, a pulse width  $\text{pw} = 2.5 \mu\text{s}$  (corresponding to a ‘liquids’ flip angle of  $33^\circ$  or a ‘solids’ flip angle of about  $90^\circ$ ) and a relaxation delay of only 1.0 s. Despite an expected quite long  $T_1(^{95}\text{Mo})$  spin-lattice relaxation time for  $\text{MoS}_2$  (see our communication), this first  $^{95}\text{Mo}$  MAS NMR experiment applied quite rapid pulsing in order to find the frequency position of the resonance for the CT. Watching the steadily improvement in S/N ratio with time, this experiment was allowed to run for about 3.5 days (i.e., acquisition of 300,000 scans) in order to achieve a decent S/N ratio. This first  $^{95}\text{Mo}$  MAS NMR spectrum showed the transmitter frequency to be somewhat offset to higher frequency compared to the center for the CT, thereby introducing quite a large intensity difference (distortion) between the two singularities for the inner  $\pm 3/2 \leftrightarrow \pm 1/2$  STs. An

expansion of the CT for this spectrum is shown in Figure S2. This highly complex spectrum formed our first challenge in extracting the  $^{95}\text{Mo}$  quadrupole coupling and CSA parameters for  $\text{MoS}_2$ . Following several trial-and-error simulations a final optimized iterative fit to the experimental spectrum resulted in the simulated spectrum shown in Figure S2 and the corresponding spectral parameters summarized in Table 1 (communication). A second and final spectrum, acquired after moving the transmitter offset to the approximate center for the CT, decreasing the pulse width to  $\text{pw} = 1.0 \mu\text{s}$  and increasing the relaxation delay to 4.0 s, is the spectrum shown in Fig. 1 (communication) and with expanded versions illustrated in Figure S3 and Figure S4. The latter spectrum in Figure S3 displays only a minor intensity distortion within the two singularities for the inner  $\pm 3/2 \leftrightarrow \pm 1/2$  STs, when compared to the simulated spectrum, a distortion which can be ascribed to a slight deviation from the ideal cable length between the probe and preamp.<sup>1</sup> Simulations show that this very complex spectrum, and in particular the spectrum for the CT, is highly sensitive to small variations in the parameters describing the quadrupole coupling and CSA tensors and the relative orientation of the two tensors. While the two Euler angles  $\psi$  and  $\zeta$  are undefined, because  $\eta_Q = \eta_\sigma = 0$ ,<sup>6</sup> the angle  $\chi$  ( $= 1^\circ \pm 8^\circ$ ) is highly sensitive to quite small variations away from the value  $\chi = 0^\circ$ . This is illustrated by the simulations in Figure S5. Thus, these two  $^{95}\text{Mo}$  tensors coincide for  $\text{MoS}_2$  and thereby reflect the cylindrical symmetry of these tensors perpendicular to the  $\text{MoS}_2$  layers.

### 3. Simulated solid-state $^{95}\text{Mo}$ MAS NMR spectra of $\text{MoS}_2$ at high field

With the high-precision values determined in this study, for both the quadrupole coupling and CSA parameters in  $\text{MoS}_2$  from  $^{95}\text{Mo}$  MAS NMR employing a mid-field (14.1 T) NMR spectrometer, it clearly would be of interest to compare the appearances of simulated high-field  $^{95}\text{Mo}$  MAS NMR spectra for  $\text{MoS}_2$  with those obtained at 14.1 T in the present study. Such a comparison is relevant for the present sample because of the opposing effects on the line broadening for the CT from the second-order quadrupole interaction (inverse proportional with

$B_0$ ) and the CSA (proportional with  $B_0$ ) and because the CSA appears to play a dominating role at least at higher magnetic fields. Simulated spectra for a spinning frequency of 5000 Hz, which illustrate the field dependence of the  $^{95}\text{Mo}$  MAS NMR spectra for  $\text{MoS}_2$  at 14.1, 19.6 and 21.1 T, are shown in Figure S6 for the relevant part of the full spectra for both the CT and all (inner and outer) of the STs, while Figure S7 shows expansions of the CT in these spectra. The spectra clearly show a broadening of the width for the CT at increasing magnetic field strength caused by the effect of the CSA. In addition, the expansions of the CT in Figure S7 illustrate that, even at 21.1 T, the quadrupole coupling constant of  $C_Q = 3.61$  MHz and the overlap with the STs still give rise to complex lineshapes for the spinning sidebands (ssbs) of the CT. Thus, it is not remarkable that the modeling of the CT, observed in a 19.6 T  $^{95}\text{Mo}$  MAS spectrum<sup>7</sup> by considering only the CSA, produce a CSA which differs substantially (by more than 20 %) from that obtained in the present study. We should note that the  $\Delta$  convention (apparently,  $\Delta = \delta_{zz} - \delta_{\text{iso}}$ ) used by these authors<sup>7</sup> for the CSA is identical to the convention used in the present work ( $\delta_{\sigma} = \delta_{\text{iso}} - \delta_{zz}$ , see section 1.3, Spectral analysis), apart from the change in sign, as we have proven from spectral simulations.

#### 4. Effect of spinning frequency on $^{95}\text{Mo}$ MAS NMR spectra of $\text{MoS}_2$ at 19.6 T

Finally, the effect of increasing the spinning frequency on the appearance of the  $^{95}\text{Mo}$  MAS spectrum of  $\text{MoS}_2$  at a high magnetic field is considered employing simulations for a field strength of 19.6 T. Simulated spectra illustrating the simplification achieved by an increase in spinning frequency as for example for 5000 Hz, 10000 Hz and 20000 Hz (i.e., taking the relevant rotor sizes/sample volumes required for  $\text{MoS}_2$  into account) are presented in Figure S8. Expansions of the CT in the three spectra are shown in Figure S9. Clearly, the simplification obtained for the  $^{95}\text{Mo}$  MAS NMR spectrum of  $\text{MoS}_2$  by increasing the spinning frequency is achieved at the expense of a loss in the content of spectral information, which is required to

determine the anisotropic parameters with high precision as illustrated in the present communication.

## 5. Conclusion

The experimental and simulated  $^{95}\text{Mo}$  MAS NMR spectra, presented above and shown below for  $\text{MoS}_2$ , illustrate that it may not always be an advantage to acquire MAS NMR spectra of a quadrupolar nucleus at the highest possible magnetic field and/or high spinning frequency when attempting to determine its anisotropic parameters with high precision.

## References:

- 1 T. Giavani, H. Bildsøe, J. Skibsted and H. J. Jakobsen, *J. Magn. Reson.*, 2004, **166**, 262.
- 2 H. J. Jakobsen, A. R. Hove, H. Bildsøe, J. Skibsted and M. Brorson, *J. Magn. Reson.*, 2007, **187**, 159.
- 3 H. J. Jakobsen, J. Skibsted, H. Bildsøe and N. C. Nielsen, *J. Magn. Reson.*, 1989, **85**, 173.
- 4 J. Skibsted, N. C. Nielsen, H. Bildsøe and H. J. Jakobsen, *J. Magn. Reson.*, 1991, **95**, 88).
- 5 Varian Manual, STARS (SpecTrum Analysis for Rotating Solids), Publication No. 87-195233-00, Rev. A0296, 1996.
- 6 J. Skibsted, N. C. Nielsen, H. Bildsøe and H. J. Jakobsen, *Chem. Phys. Lett.*, 1992, **188**, 405.
- 7 J.-B. d'Espinose de Lacaillerie and Z. Gan, *Appl. Magn. Reson.*, 2007, **32**, 499.

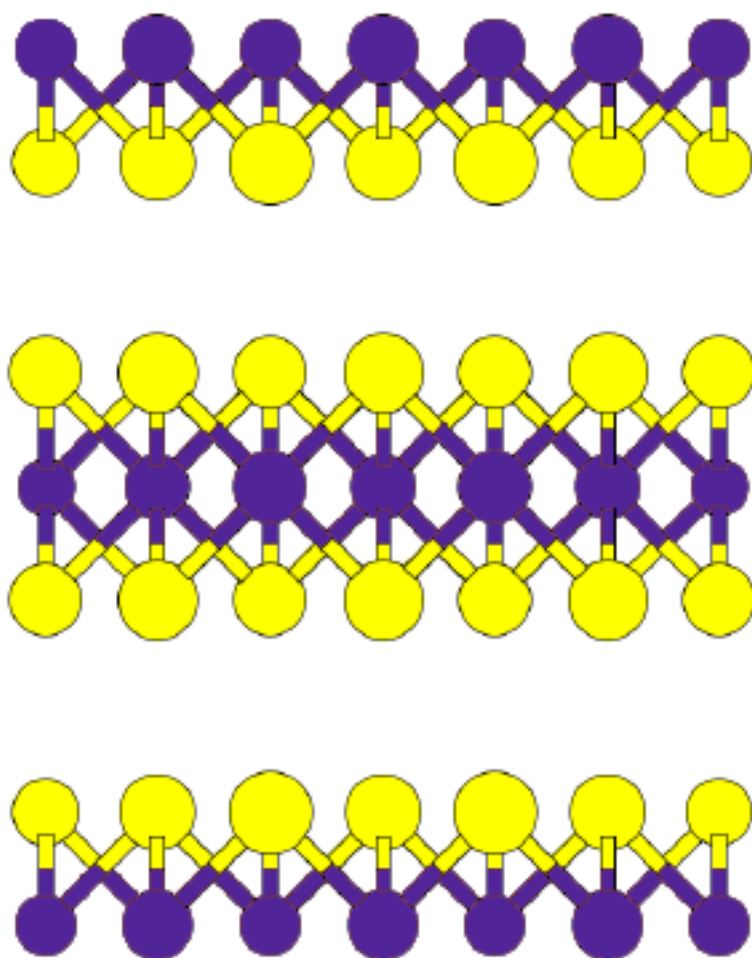


**Figure S1.** The layer structure for MoS<sub>2</sub>. Mo (blue) and S (yellow).



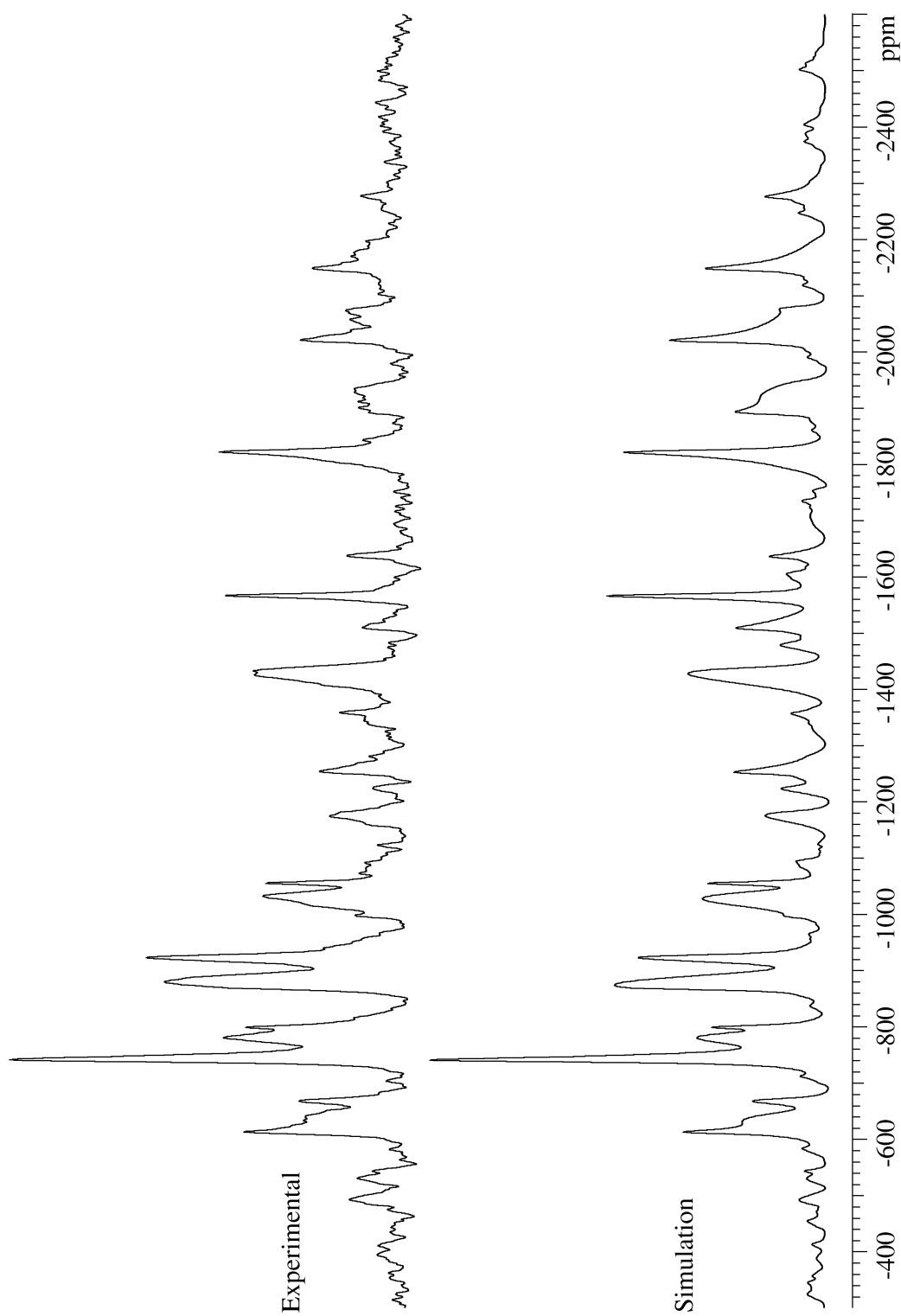


**Figure S2.** First  $^{95}\text{Mo}$  MAS NMR spectrum for the CT in  $\text{MoS}_2$  (see text).

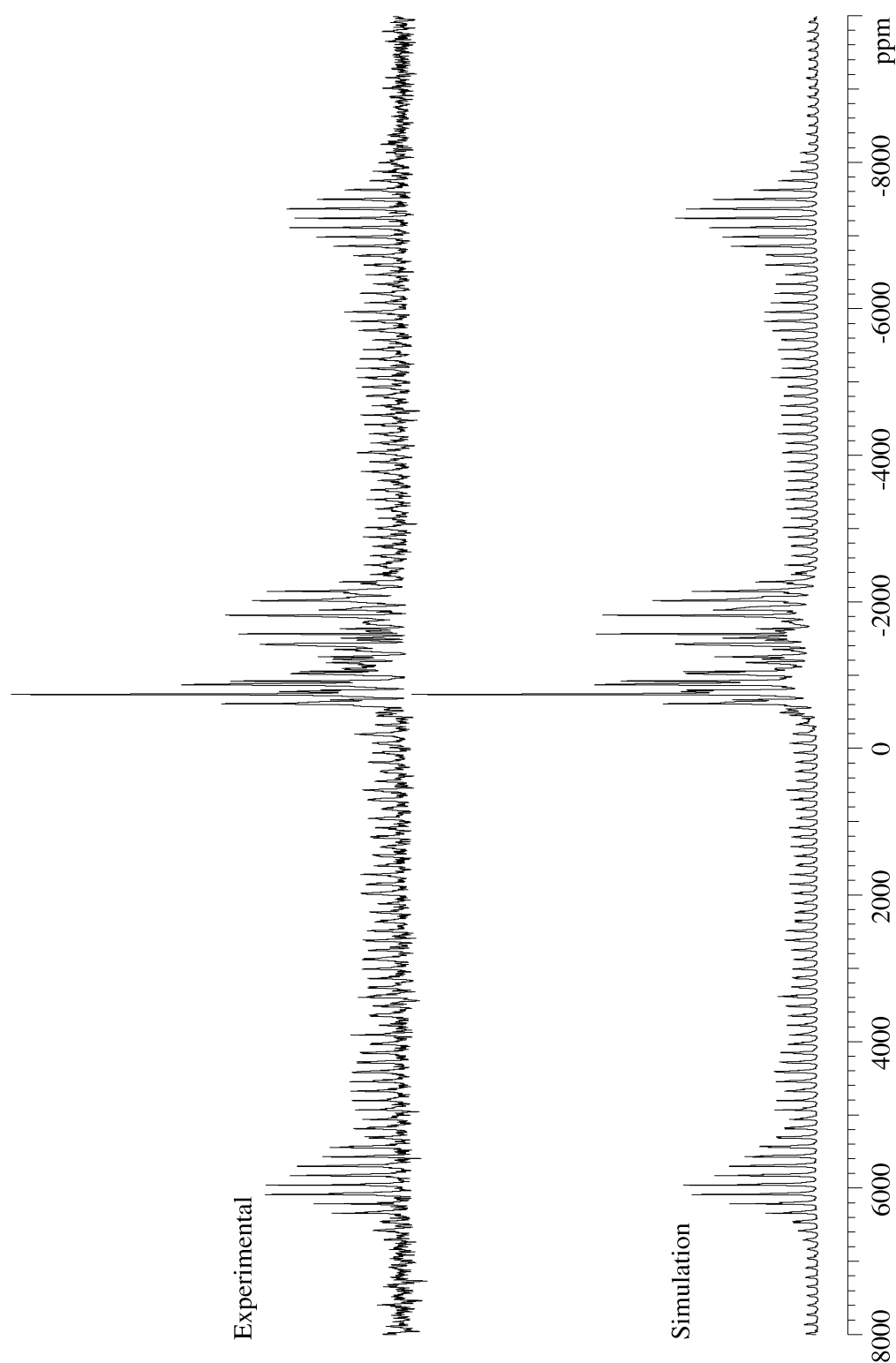


**Figure S3.** Optimum and second  $^{95}\text{Mo}$  MAS NMR spectrum obtained, which shows the CT and inner STs for  $\text{MoS}_2$ . The spectra are an expansion of those shown in Fig. 1 of the original communication.

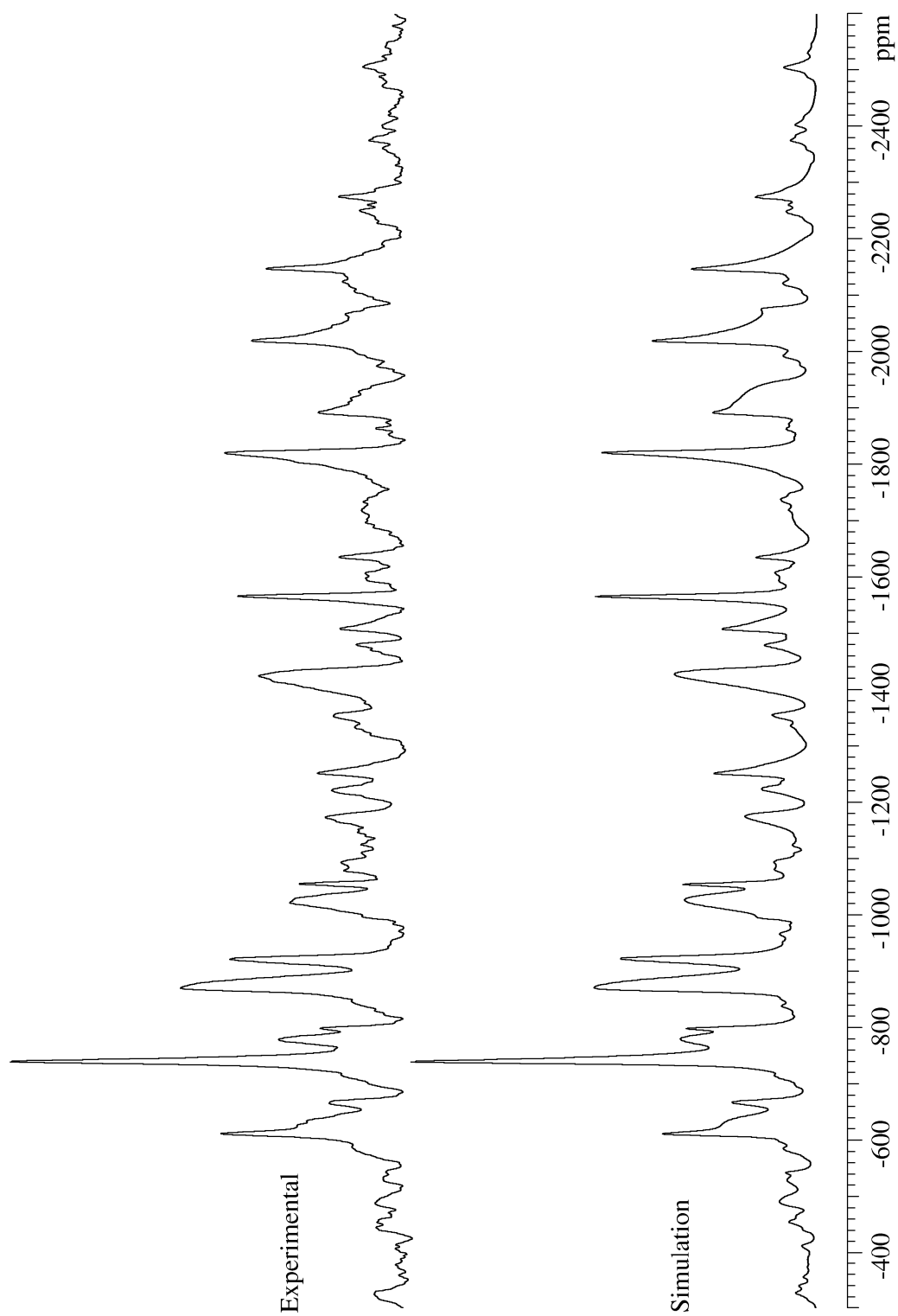


**Figure S4.** Expansions of the CT for the  $^{95}\text{Mo}$  MAS NMR spectra of  $\text{MoS}_2$  in Figure S3 are shown.

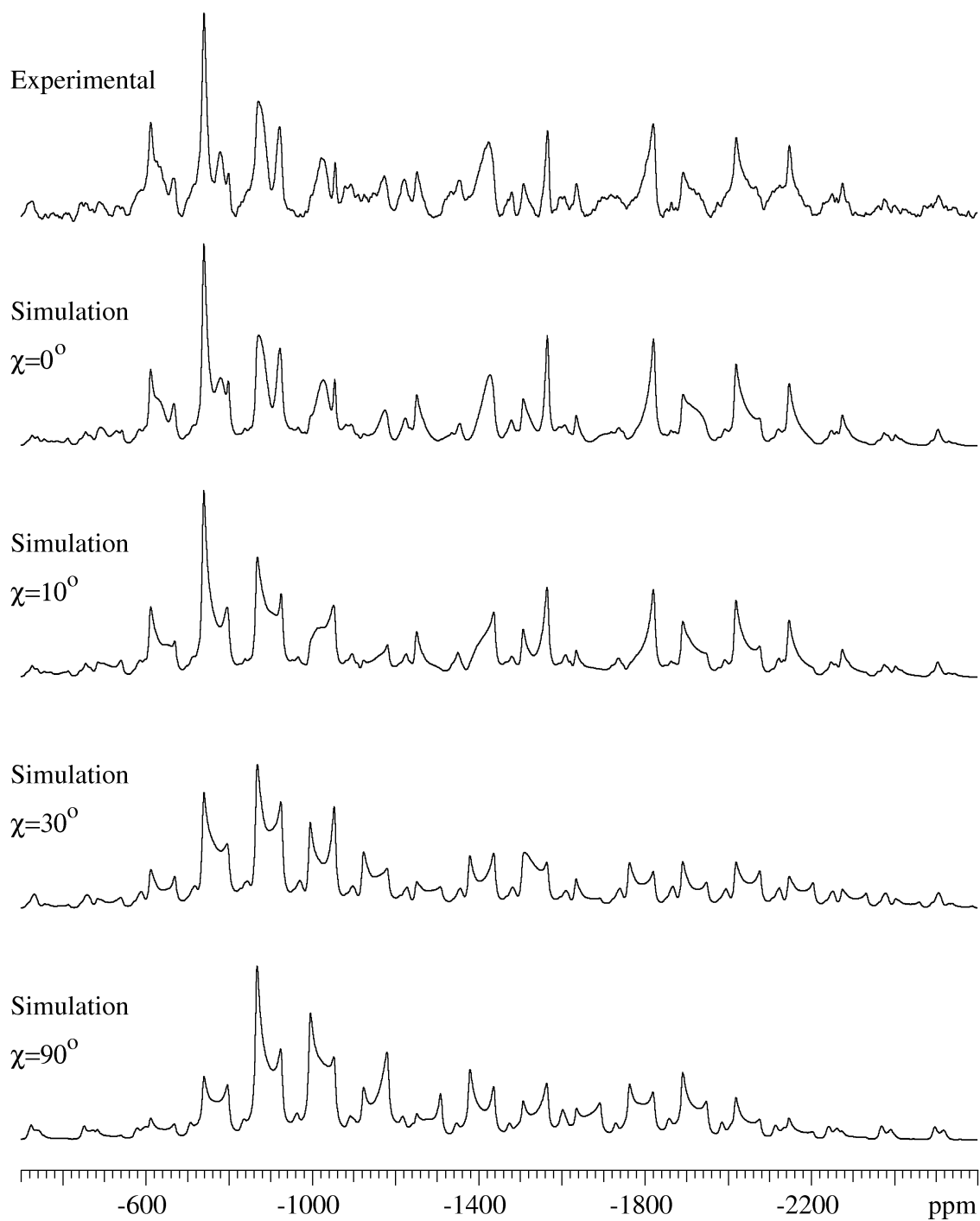


**Figure S5.** Simulations, which show the dependence on the Euler angle  $\chi$  for the CT in the  $^{95}\text{Mo}$  MAS NMR spectrum of  $\text{MoS}_2$ , are illustrated (see text).

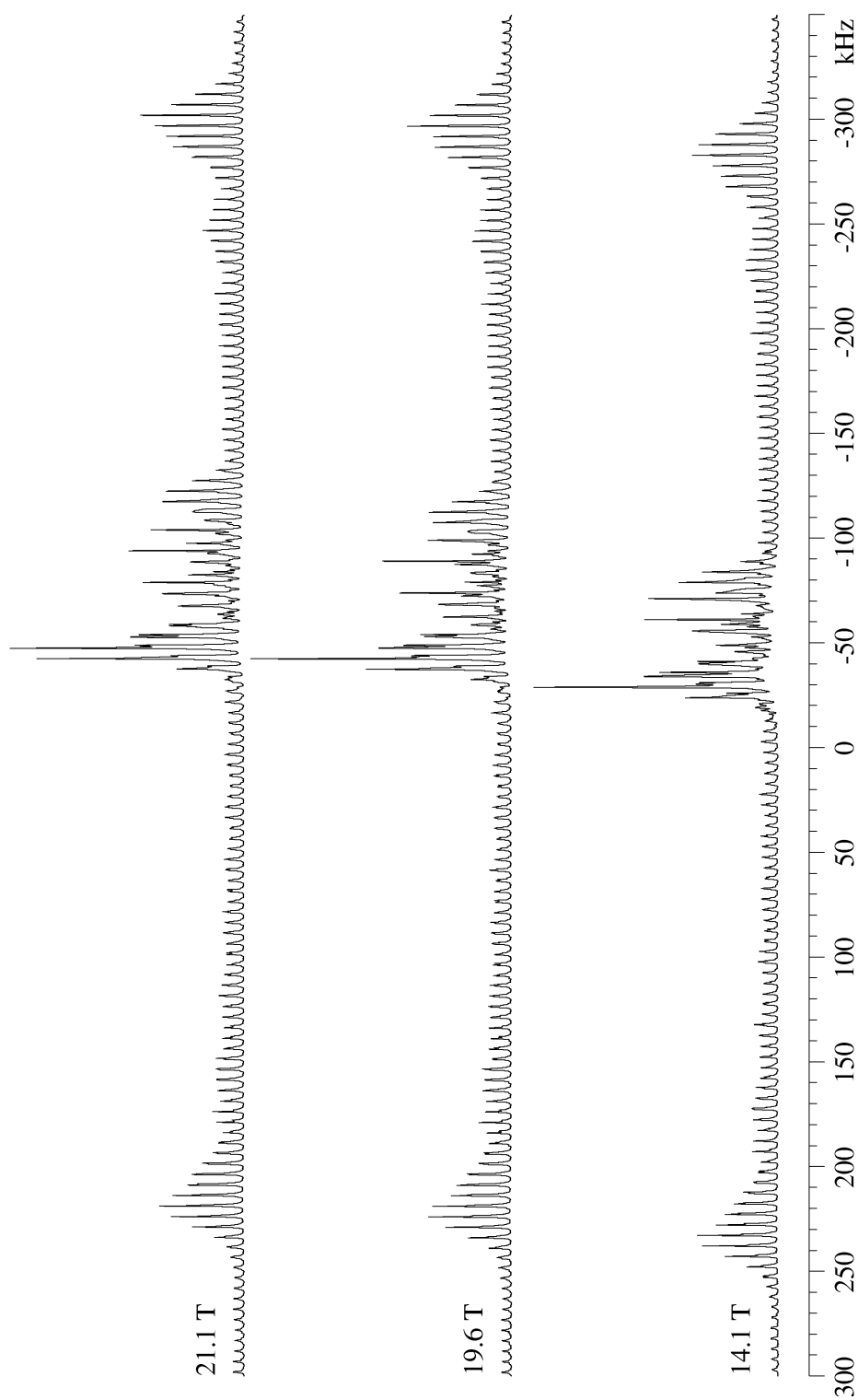


**Figure S6.** Simulated  $^{95}\text{Mo}$  MAS NMR spectra of  $\text{MoS}_2$  for three magnetic field strengths.

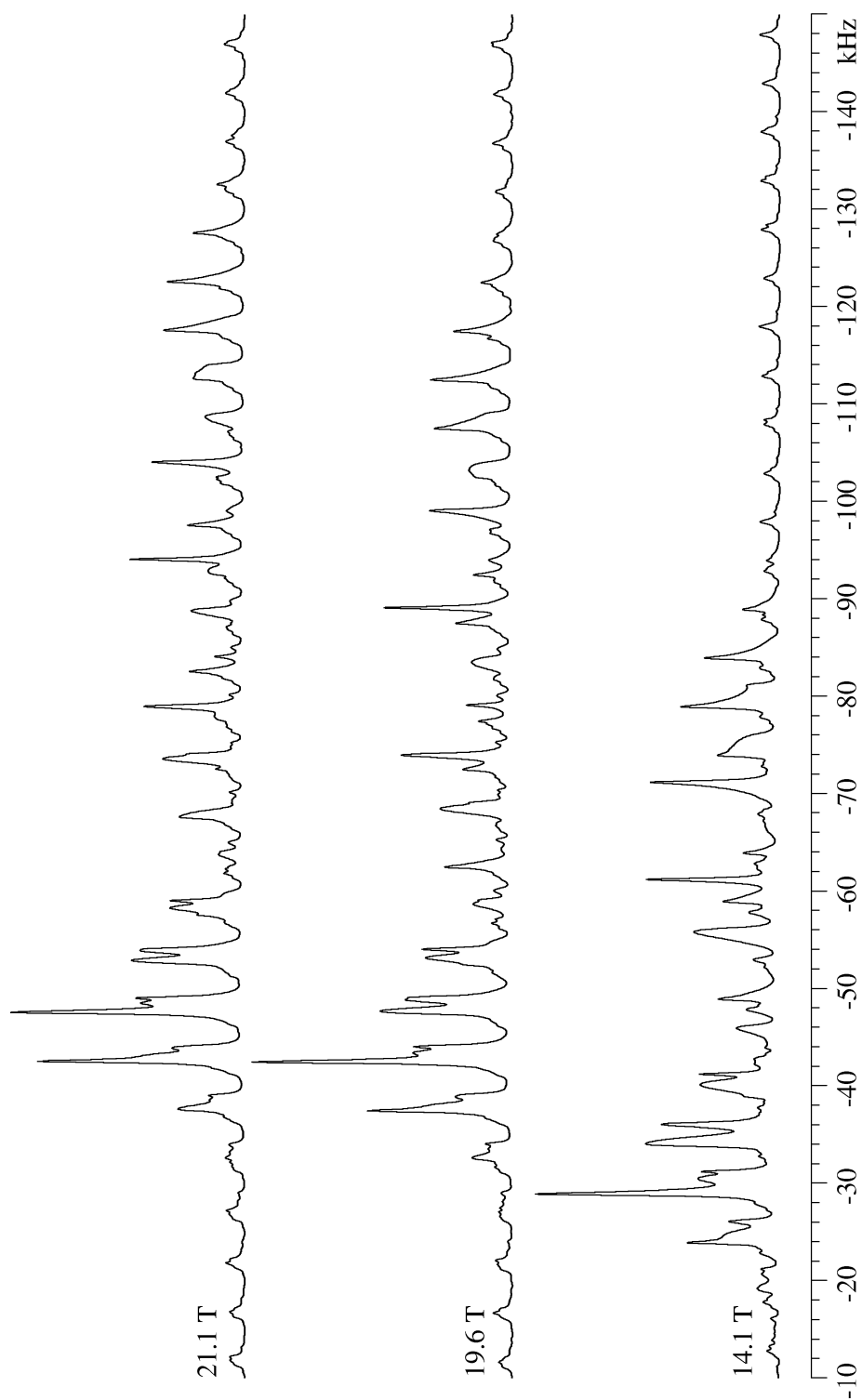


**Figure S7.** Expansions for the CT from the three  $^{95}\text{Mo}$  MAS NMR spectra of  $\text{MoS}_2$  simulated for the three magnetic field strengths in Figure S6.

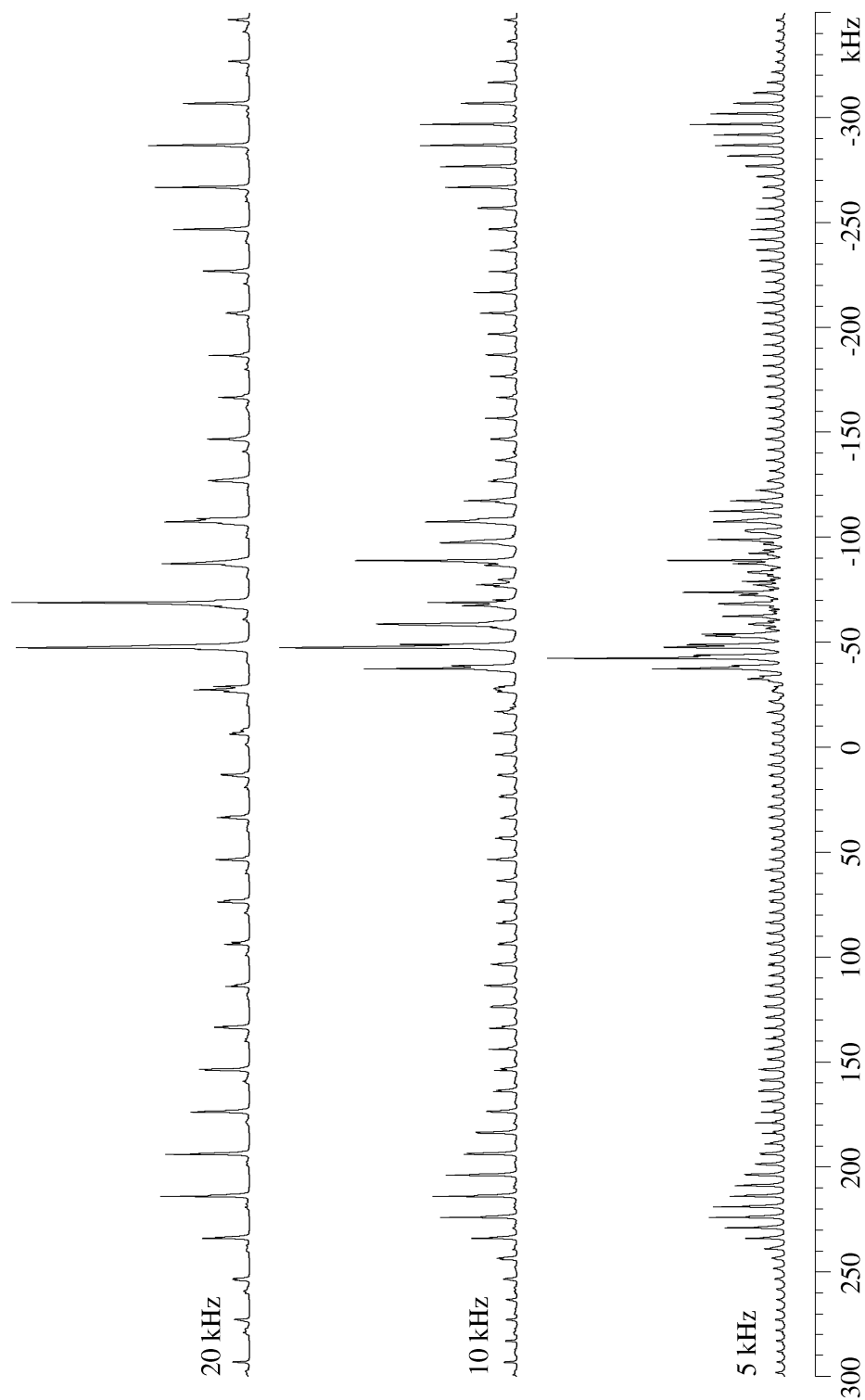


**Figure S8.** Simulations are illustrated for the effects of spinning frequency on <sup>95</sup>Mo MAS NMR spectra of MoS<sub>2</sub> at 19.6 T for three different spinning frequencies.

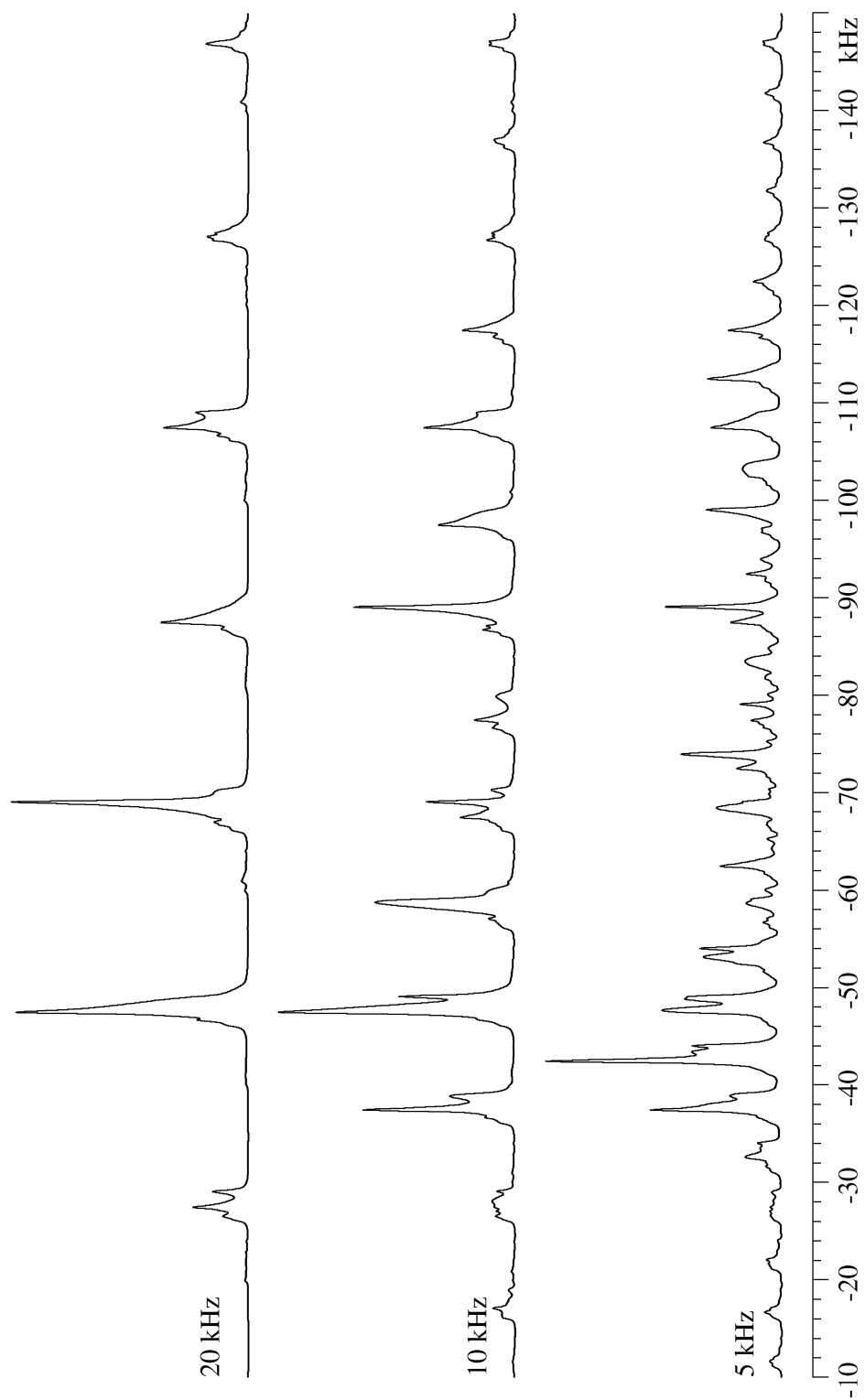


**Figure S9.** Expansions for the CT from the three  $^{95}\text{Mo}$  MAS NMR spectra of  $\text{MoS}_2$  simulated for the three spinning frequencies in Figure S8.